

$\pi^+\pi^-$ emission from coherent ρ^0 propagation in nuclei

Swapan Das*

Nuclear Physics Division, Bhabha Atomic Research Centre, Mumbai-400085, India

(Received 19 August 2005; published 29 December 2005)

Cross sections for the $\pi^+\pi^-$ events arising from the decay of the ρ^0 meson have been calculated. This ρ meson is considered to be produced coherently in the (p, p') reaction in a nucleus. The distorted-wave functions for the continuum particles and the ρ meson propagator are described by the eikonal form. The sensitivity of the cross section to the pion emission angle as well as to the beam energy has been investigated. The cross sections for the ρ^0 meson decaying inside and outside the nucleus are compared. In addition, the coherent and incoherent contributions to the cross section due to ρ^0 inside and outside decay amplitudes are presented. The initial- and final-state interactions for this reaction have been studied. The nuclear medium effect on ρ^0 -meson propagation through the nucleus is also explored.

DOI: 10.1103/PhysRevC.72.064619

PACS number(s): 25.40.Ve

I. INTRODUCTION

The hadron parameters for vector mesons embedded in the nucleus may differ significantly from their free-space values because of the interaction that has taken place between the vector mesons and the other nuclear particles present in the nucleus. Therefore, the study of the in-medium properties of vector mesons can offer valuable information about vector meson dynamics in a nucleus. In compressed [$\rho \approx (3-5)\rho_0$] and/or hot [$\sim(150-200)$ MeV] nuclei, the medium effect on the vector meson could be drastic. In fact, a large medium effect on the ρ meson is believed to be seen in the enhanced dilepton yield in CERES and HELIOS ultrarelativistic heavy-ion collision data [1] taken in CERN-SPS. Theoretically, these data are found to be compatible if the ρ mass is reduced drastically, i.e., by $\sim 300-400$ MeV [2]. In contrast, these data are also reproduced successfully by calculations [3] that incorporate the hadronic interaction for the ρ meson with the surrounding nuclear particles. Recent analysis on the $\pi^+\pi^-$ pairs, in the STAR experiment at BNL RHIC, showed a decrease in ρ mass in the peripheral Au + Au collisions [4].

There exist some model calculations which envisage the reduction of vector meson mass in the nuclear medium. For example, the scaling hypothesis due to Brown and Rho [5] shows that the mass of the vector meson in a nucleus should drop, since the pion weak decay constant does. The QCD sum rule calculation done by Hatsuda and Lee [6] shows that the reduction in the vector meson mass increases with the nuclear density. This finding is also corroborated by the vector dominance model (VDM) calculation due to Asakawa *et al.* [7]. The quark meson (QM) coupling model calculation done by Saito *et al.* [8] shows that the mass of ρ meson in the ^{12}C nucleus is reduced by 50 MeV. Besides these, the many-body calculations show that the spectral function for the ρ meson in the nuclear medium is significantly modified because of its interaction with the nucleon and resonances. In one of these calculations, Friman *et al.* [9] showed that the p -wave ρN scattering [via $N(1720)$ and $\Delta(1905)$ resonances]

reduces the mass of the ρ meson, and this reduction is significant at high baryon densities. Peters *et al.* [10] have extended this calculation by incorporating all four starred s - and p -wave resonances. Their calculations show a strong influence of the s -wave resonances on the ρ spectral function, specifically in the static limit. The density-dependent two-pion self-energy calculation due to Herrmann *et al.* [11] shows an enhancement in the in-medium ρ width, but unlike others, they have not found any significant change in the in-medium ρ mass. The recent developments in this field are illustrated in Ref. [12].

To look for the in-medium properties of vector mesons in a normal nucleus, experimental programs are under way at various centers around the world. For example, there are proposals to measure the photoproduction of vector mesons in the nucleus at TJNAF through e^+e^- radiation [13] and at the 1.3 GeV Tokyo Electron Synchrotron (INS) through $\pi^+\pi^-$ emission [14]. Recently, the CBELSA/TAPS Collaboration at ELSA [15] found the medium effect on the ω meson in the ^{93}Nb nucleus. The KEK-PS E325 Collaboration at KEK [16] measured the e^+e^- yield in the $p + A$ reaction at 12 GeV, and they reported an enhancement in this yield in the region of $0.6 \geq m_{e^+e^-} \leq 0.77$ GeV/ c^2 due to modified ρ meson in the nuclei. Another experiment [17] in this collaboration (which investigates the medium effect on ϕ mesons) is in progress. There are also experimental programs at GSI-SIS [18] (the HADE Collaboration) as well as at Spring-8 RCNP [19], which are dedicated to explore the hadron parameters for vector mesons in the normal nucleus. Therefore, an overall view of the medium effect on vector mesons is expected in the near future.

There also exist several calculations showing the medium effect on vector mesons in the normal nucleus. Eletsky *et al.* [20] and Kondratyuk *et al.* [21] related the effective mass and width for the ρ meson in a nucleus to the ρ nucleon scattering amplitude $f_{\rho N}$ and nuclear density. In their calculations it was shown that the mass of the ρ meson in a normal nucleus increases with its energy. In the static limit, the ρ mass is below its free-space value, where as it exceeds 770 MeV at higher energies [21]. Effenberger *et al.* studied e^+e^- production from the γ - [22] and pion- [23] induced nuclear reactions

*Electronic address: swapand@apsara.barc.ernet.in

at GeV energies in the framework of the semiclassical Boltzmann-Uehling-Uhlenbeck (BUU) transport model. Their study shows that the medium modification of vector mesons enhances the dilepton yields in the e^+e^- invariant mass region below 770 MeV. The intranuclear cascade (INC) model calculation, due to Golubeva *et al.* [24], also supports this conclusion. Several studies [25] show that the width of ϕ meson in a nucleus increases significantly, whereas its mass shift is insignificant.

Another way to explore the ρ dynamics in a normal nucleus could be through coherent ρ^0 production in the (p, p') reaction. The coherent meson production process has been used to unveil many interesting aspects of the nuclear dynamics. For example, the pion and Δ dynamics in a nucleus were investigated in the past through the coherent photoproduction and electroproduction of pions in the Δ excitation region [26–28]. In this energy region, the measurements had been done on coherent π^+ production in the charge-exchange reactions [29]. These reactions offer valuable informations [30] which are complementary to those obtained from the scattering of real pions on a nucleus [26,27].

For coherent ρ^0 emission in the (p, p') reaction, it is envisaged that the beam proton emits a ρ meson. This ρ meson, of course, is a virtual particle, since the four-momentum carried by it is constrained by the dispersion relation obeyed by protons. It is the nucleus that scatters this ρ^0 meson coherently and brings it on shell. Kinematically, this process is possible because the recoiling nucleus, as a whole, can adjust the momentum to put the virtual ρ meson on its mass shell. For simplicity, we restrict the propagation of the coherent ρ^0 meson to the forward direction only. This ρ meson, after traveling a certain distance, decays into π^+ and π^- in the final state. Naturally, the ρ^0 dynamics in this reaction can be manifested from these $\pi^+\pi^-$ events. Therefore, the coherent ρ meson production process can be considered an appropriate probe to acquire knowledge about the ρ and nucleus interaction.

The energy transfer $E_p - E_{p'}$ distribution spectra have been calculated for the $(p, p'[\pi^+\pi^-])$ reaction on various nuclei. According to the model presented here, the $\pi^+\pi^-$ events in the final state arise owing to the decay of coherent ρ^0 meson, propagating through a nucleus. This calculation is based on the Glauber approach for the nuclear effect, where the distorted-wave functions for the continuum particles (i.e., p, p', π^+ , and π^-) and the ρ^0 propagator have been described by the eikonal form. The potential necessary to generate these quantities is constructed by using the tQ approximation. In this study the dependence of the cross section on the pion emission angle as well as on the beam energy is presented. The cross sections for the ρ meson decaying inside and outside the nucleus are compared. Along with this, the coherent and incoherent contributions to the cross section due to inside and outside decay for the ρ meson are also studied. The initial- and final-state interactions for this reaction are investigated. In addition, the medium effect on the ρ meson propagating through the nucleus is explored.

We write the formalism in Sec. II for coherent ρ meson production in the (p, p') reaction and its decay into π^+ and π^- in the final state. The results and discussion for this reaction

are illustrated in Sec. III. Conclusions obtained from this study have been presented in Sec. IV.

II. FORMALISM

The formalism for the $\pi^+\pi^-$ emission from the ρ meson, propagating through a nucleus, has been developed here. This ρ meson is produced coherently in the (p, p') reaction in a nucleus. The T matrix T_{fi} for this reaction consists of production, propagation, and decay (into two pions) for the ρ meson, i.e.,

$$T_{fi} = \int \int d\mathbf{r} d\mathbf{r}' \chi^{(-)*}(\mathbf{k}_{\pi^+}, \mathbf{r}') \chi^{(-)*}(\mathbf{k}_{\pi^-}, \mathbf{r}) \times \Gamma_{\rho\pi\pi} S_{\rho}(\mathbf{r}' - \mathbf{r}) \Psi_{\rho^0}(\mathbf{r}). \quad (1)$$

The factor $\Psi_{\rho^0}(\mathbf{r})$ in the above equation represents the ρ^0 production amplitude due to the (p, p') reaction. It is given by

$$\Psi_{\rho^0}(\mathbf{r}) = \Pi_{\rho}(q_0, \mathbf{r}) G_{\rho}(q^2) \chi^{(-)*}(\mathbf{k}_p, \mathbf{r}) \Gamma_{\rho NN} \chi^{(+)}(\mathbf{k}_p, \mathbf{r}), \quad (2)$$

where $\Pi_{\rho}(q_0, \mathbf{r}) [= 2q_0 V_{O\rho}(\mathbf{r})]$ denotes the self-energy for the ρ meson, arising because of the ρ nucleus optical potential $V_{O\rho}(\mathbf{r})$. This potential describes the elastic scattering of the virtual ρ meson to its real state. $q_0 (= E_p - E_{p'})$ is the energy carried out by the virtual ρ meson. $\bar{G}_{\rho}(q^2)$ represents the propagator for the virtual ρ meson emitted at the $\rho^0 pp'$ vertex: $\bar{G}_{\rho}(q^2) = -1/(m_{\rho}^2 - q^2)$. Here, m_{ρ} (~ 770 MeV) and q ($= k_p - k_{p'}$) are the mass and the four-momentum, respectively, for the ρ meson. In Eq. (2), χ s denote the distorted-wave functions for protons. In eikonal approximation, they can be written as

$$\chi^{(+)}(\mathbf{k}_p, \mathbf{r}) = \exp(i\mathbf{k}_p \cdot \mathbf{r}) \exp\left[-\frac{i}{v_p} \int_{-\infty}^z dz' V_{O\rho}(\mathbf{b}, z')\right],$$

and

$$\chi^{(-)*}(\mathbf{k}_{p'}, \mathbf{r}) = \exp(-i\mathbf{k}_{p'} \cdot \mathbf{r}) \exp\left[-\frac{i}{v_{p'}} \int_z^{\infty} dz' V_{O\rho'}(\mathbf{b}, z')\right]. \quad (3)$$

$\Gamma_{\rho NN}$, in Eq. (2), is the vertex function at the $\rho^0 pp'$ vertex. It describes the emission of the virtual ρ^0 at this vertex. The Lagrangian, describing the interaction at the ρNN vertex, is given by

$$\mathcal{L}_{\rho NN} = -g_V F(q^2) \bar{N} \left[\gamma^{\mu} - i \frac{\kappa}{2m_N} \sigma^{\mu\nu} q_{\nu} \right] \tau \cdot \rho_{\mu} N, \quad (4)$$

with $g_V = 2.6$ and $\kappa = 6.1$ [26]. $F(q^2)$ represents the form factor at the ρNN vertex: $F(q^2) = (\Lambda^2 - m_{\rho}^2)/(\Lambda^2 - q^2)$, with $\Lambda = 1.3$ GeV/c [31]. The quantities m_{ρ} and q are already defined below Eq. (2).

The factor $S_{\rho}(\mathbf{r}' - \mathbf{r})$, appearing in Eq. (1), describes the propagation for the real ρ^0 meson from position \mathbf{r} to another position \mathbf{r}' , which, in the present work, has been restricted to the forward direction only. Therefore, $S_{\rho}(\mathbf{r}' - \mathbf{r})$ can be expressed in the eikonal form as

$$S_{\rho}(\mathbf{r}' - \mathbf{r}) = \delta(\mathbf{b}' - \mathbf{b}) \Theta(z' - z) \times \exp[i\mathbf{k}_{\rho} \cdot (\mathbf{r}' - \mathbf{r})] D_{\mathbf{k}_{\rho}}(\mathbf{b}, z', z), \quad (5)$$

where $D_{\mathbf{k}_\rho}(\mathbf{b}, z', z)$ describes the nuclear medium effect on ρ propagation through a nucleus. It is given by

$$D_{\mathbf{k}_\rho}(\mathbf{b}, z', z) = -\frac{i}{2k_\rho} \exp\left\{\frac{i}{2k_\rho} \times \int_z^{z'} dz'' [\tilde{G}_{0\rho}^{-1}(m) - 2E_\rho V_{O\rho}(\mathbf{b}, z'')]\right\}. \quad (6)$$

In this equation, k_ρ is the momentum for the forward-going ρ meson. $V_{O\rho}(\mathbf{b}, z'')$, as mentioned above, represents the optical potential for the ρ meson. $\tilde{G}_{0\rho}^{-1}(m)$ represents the inverse of the free ρ meson (on-shell) propagator. It is given by

$$\tilde{G}_{0\rho}^{-1}(m) = m^2 - m_\rho^2 + im_\rho \Gamma_\rho(m), \quad (7)$$

$$\Gamma_\rho(m) = \Gamma_\rho(m_\rho) \left(\frac{m_\rho}{m}\right) \left[\frac{k(m^2)}{k(m_\rho^2)}\right]^3,$$

with $m_\rho \approx 770$ MeV and $\Gamma_\rho(m_\rho) \sim 150$ MeV, for $\rho^0 \rightarrow \pi^+\pi^-$ in the free state. $k(m^2)$ is the momentum for the pion in the rest frame of the decaying ρ meson of mass m .

$\Gamma_{\rho\pi\pi}$, in Eq. (1), describes the vertex function for the ρ^0 meson decaying into $\pi^+\pi^-$ in the final state. It is governed by the Lagrangian

$$\mathcal{L}_{\rho\pi\pi} = f_{\rho\pi\pi} \rho^\mu \cdot (\pi \times \partial_\mu \pi), \quad (8)$$

with $f_{\rho\pi\pi} \approx 6.1$ [26,32].

The distorted-wave functions χ s, in Eq. (1), for pions in the final state have been described by the eikonal form, i.e.,

$$\chi^{(-)*}(\mathbf{k}_{\pi^+}, \mathbf{r}') \chi^{(-)*}(\mathbf{k}_{\pi^-}, \mathbf{r}') = \exp[-i(\mathbf{k}_{\pi^+} + \mathbf{k}_{\pi^-}) \cdot \mathbf{r}'] D_{\mathbf{k}_\pi}(\mathbf{b}', z'). \quad (9)$$

In this equation, $D_{\mathbf{k}_\pi}(\mathbf{b}', z')$ represents the distortion occurring because of the elastic scattering of pions by the recoiling nucleus. It is given by

$$D_{\mathbf{k}_\pi}(\mathbf{b}', z') = \exp\left\{-i \int_{z'}^\infty dz'' \left[\frac{V_{O\pi^+}(\mathbf{b}', z'')}{v_{\pi^+}} + \frac{V_{O\pi^-}(\mathbf{b}', z'')}{v_{\pi^-}} \right]\right\}, \quad (10)$$

where v_{π^\pm} is the velocity of π^\pm and $V_{O\pi^\pm}(\mathbf{b}', z')$ denotes the optical potential for the π^\pm scattering in a nucleus.

The T matrix T_{fi} , given in Eq. (1), can be factorized into interaction and structure parts. The interaction part contains the production and decay vertex functions (i.e., $\Gamma_{\rho NN} \Gamma_{\rho\pi\pi}$) for the ρ meson. The structure part carries the information about the medium effect on the ρ meson. The latter, from Eqs. (1), (5), and (9), can be written as

$$F = \int d\mathbf{r} D_{\pi\rho}(\mathbf{k}_\pi, \mathbf{k}_\rho; \mathbf{b}, z) \exp(-i\mathbf{k}_\rho \cdot \mathbf{r}) \times \Pi_\rho(q_0, \mathbf{r}) \tilde{G}_\rho(q^2) \chi^{(-)*}(\mathbf{k}_p, \mathbf{r}) \chi^{(+)}(\mathbf{k}_p, \mathbf{r}), \quad (11)$$

with $\mathbf{k}_\rho = \mathbf{k}_{\pi^+} + \mathbf{k}_{\pi^-}$. The symbol $D_{\pi\rho}(\mathbf{k}_\pi, \mathbf{k}_\rho; \mathbf{b}, z)$ appearing in this equation stands for

$$D_{\pi\rho}(\mathbf{k}_\pi, \mathbf{k}_\rho; \mathbf{b}, z) = \int_z^\infty dz' D_{\mathbf{k}_\pi}(\mathbf{b}, z') D_{\mathbf{k}_\rho}(\mathbf{b}, z', z), \quad (12)$$

where $D_{\mathbf{k}_\rho}(\mathbf{b}, z', z)$ and $D_{\mathbf{k}_\pi}(\mathbf{b}, z')$ are defined in Eqs. (6) and (10), respectively. The above equation describes the dynamics for the π and ρ mesons in the nucleus.

The ρ meson, due to its short lifetime ($\sim 10^{-23}$ s), can decay inside as well as outside the nucleus, depending on its velocity and the size of the nucleus. Indeed, the physical quantity that determines this decay probability is the effective decay length: $\lambda^* = v/\Gamma^*$, where v and Γ^* describe the velocity and the effective decay width, respectively, for the ρ meson in a nucleus. This decay length λ^* controls the attenuation for the in-medium ρ propagation. While the ρ meson propagates a distance $L(\mathbf{b}, z) [= \sqrt{R^2 - b^2} - z]$ from production point z to the surface of a nucleus of radius R , it is attenuated by a factor $\exp[-L(\mathbf{b}, z)/\lambda^*]$. To investigate the inside and outside decay probabilities more transparently, $D_{\pi\rho}(\mathbf{k}_\pi, \mathbf{k}_\rho; \mathbf{b}, z)$ in Eq. (12) is split into two parts, i.e.,

$$D_{\pi\rho}(\mathbf{k}_\pi, \mathbf{k}_\rho; \mathbf{b}, z) = D_{\pi\rho}^{\text{in}}(\mathbf{k}_\pi, \mathbf{k}_\rho; \mathbf{b}, z) + D_{\pi\rho}^{\text{out}}(\mathbf{k}_\pi, \mathbf{k}_\rho; \mathbf{b}, z). \quad (13)$$

In this equation, $D_{\pi\rho}^{\text{in}}(\mathbf{k}_\pi, \mathbf{k}_\rho; \mathbf{b}, z)$ and $D_{\pi\rho}^{\text{out}}(\mathbf{k}_\pi, \mathbf{k}_\rho; \mathbf{b}, z)$ correspond to the probabilities for the ρ meson decaying inside and outside the nucleus, respectively. They are given by

$$D_{\pi\rho}^{\text{in}}(\mathbf{k}_\pi, \mathbf{k}_\rho; \mathbf{b}, z) = \int_z^{\sqrt{R^2 - b^2}} dz' D_{\mathbf{k}_\pi}(\mathbf{b}, z') D_{\mathbf{k}_\rho}(\mathbf{b}, z', z) \quad (14)$$

and

$$D_{\pi\rho}^{\text{out}}(\mathbf{k}_\pi, \mathbf{k}_\rho; \mathbf{b}, z) = \int_{\sqrt{R^2 - b^2}}^\infty dz' D_{\mathbf{k}_\pi}(\mathbf{b}, z') D_{\mathbf{k}_\rho}(\mathbf{b}, z', z). \quad (15)$$

In Eq. (15), $D_{\mathbf{k}_\pi}(\mathbf{b}, z')$ goes to unity, and $D_{\mathbf{k}_\rho}(\mathbf{b}, z', z)$ reduces to $-(i/2k_\rho) \exp[(i/2k_\rho) \tilde{G}_{0\rho}^{-1}(m_\rho)(z' - z)]$.

For the $\pi^+\pi^-$ emission in the (p, p') reaction on a nucleus, the differential cross section for the energy transfer $E_p - E_{p'}$ distribution can be written as

$$\frac{d\sigma}{dE_{p'} d\Omega_{p'} dE_{\pi^+} d\Omega_{\pi^+} d\Omega_{\pi^-}} = \frac{\pi^3}{(2\pi)^{11}} \frac{m_p^2 k_{p'} k_{\pi^+} k_{\pi^-}}{k_p} \langle |T_{fi}|^2 \rangle. \quad (16)$$

The angle bracket around $|T_{fi}|^2$ represents the average over the spin orientations of the particles in the initial state and the summation over the spin orientations of the particles in the final state.

III. RESULTS AND DISCUSSION

To calculate the T matrix T_{fi} , given in Eq. (1), it is necessary to evaluate the wave functions for protons in Eq. (3) and pions in Eq. (9), as well as the propagator for the ρ meson in Eq. (5). The important ingredient required for generating these quantities is the optical potential for the respective particles. This potential, in the present work, has been estimated by using the tQ approximation. According to it, the optical potential $V_{OX}(\mathbf{r})$ for a particle X scattered by a nucleus can be expressed [33] as

$$V_{OX}(\mathbf{r}) = -\frac{v_X}{2} (i + \alpha_{XN}) \sigma_i^{XN} \varrho(\mathbf{r}); \quad (17)$$

α_{XN} appearing in this equation denotes the ratio $\text{Re}f_{XN}(0)/\text{Im}f_{XN}(0)$. Here, $f_{XN}(0)$ is the particle-nucleon ($X - N$) scattering amplitude in the forward direction. σ_t^{XN} represents the total scattering cross section. $\varrho(\mathbf{r})$ denotes the spatial distribution for the nuclear density, usually approximated by the charge density distribution for the nucleus. The present work deals with ^{12}C and ^{208}Pb nuclei only. Therefore, the form of $\varrho(\mathbf{r})$ for these nuclei, as extracted from the electron scattering data [34], is given by,

$$\text{for } ^{12}\text{C}, \quad \varrho(\mathbf{r}) = \varrho_0[1 + w(r/c)^2]e^{-(r/c)^2}, \quad w = 1.247, \\ c = 1.649 \text{ fm}; \quad (18)$$

$$\text{for } ^{208}\text{Pb}, \quad \varrho(\mathbf{r}) = \varrho_0 \frac{1 + w(r/c)^2}{1 + \exp\left(\frac{r^2 - c^2}{a^2}\right)}; \quad w = 0.3379, \\ c = 6.3032 \text{ fm}, \quad a = 2.8882 \text{ fm}. \quad (19)$$

These densities are normalized to the mass numbers of the corresponding nuclei.

To evaluate the proton nucleus optical potential $V_{Op}(\mathbf{r})$ in Eq. (17), the energy-dependent measured values for the proton-nucleon scattering parameters, i.e., α_{pN} and σ_t^{pN} [35,36], have been used. Similarly, $\alpha_{\pi^{\pm}N}$ and $\sigma_t^{\pi^{\pm}N}$ are used as input quantities in Eq. (17) to generate the π^{\pm} nucleus optical potential $V_{O\pi^{\pm}}(\mathbf{r})$. The data for $\sigma_t^{\pi^{\pm}p}$ exist for a wide range of energies [36]. The measured values for $\alpha_{\pi^{\pm}p}$ are also available in Ref. [36] at higher energies only. Therefore, $\alpha_{\pi^{\pm}p}$ has been generated at lower energies by using the SAID program [37]. For π^{\pm} neutron scattering parameters, they are approximated as $\alpha_{\pi^{\pm}n} \approx \alpha_{\pi^{\pm}p}$ and $\sigma_t^{\pi^{\pm}n} \approx \sigma_t^{\pi^{\pm}d} - \sigma_t^{\pi^{\pm}p}$. The data for the pion-deuteron total scattering cross section $\sigma_t^{\pi^{\pm}d}$ are also available in Ref. [36].

The ρ meson, being an unstable particle, cannot exist as a beam. Therefore, α_{ρ^0N} and $\sigma_t^{\rho^0N}$ [which are required in Eq. (17) for estimating the ρ^0 nucleus optical potential $V_{O\rho}(\mathbf{r})$] cannot be measured directly. On the other hand, they can be extracted from the ρ production data available for various elementary reactions. In fact, several authors have done this exercise recently for a wide range of ρ energies. In one of these calculations, using vector dominance model (VDM), Kondratyuk *et al.* [21] extracted the ρ nucleon scattering amplitude $f_{\rho N}$ from the ρ -meson photoproduction data at higher energies ($E_\rho \geq 2 \text{ GeV}$). At lower energies ($E_\rho \leq 2 \text{ GeV}$) they calculated $f_{\rho N}$ by using the resonance model (RM), since the ρ meson couples strongly to a number of resonances in this energy region. In another calculation Lutz *et al.* used the coupled-channel approach [38] to calculate $f_{\rho N}$ in the region of threshold ρ production. In this energy region, their calculations reproduce the measured cross sections for various reactions, such as $\pi N \rightarrow \rho N$ and $\gamma N \rightarrow \rho N$, very well.

As mentioned above, we calculate the energy transfer $E_p - E_{p'}$ distribution spectra for the $\pi^+\pi^-$ emission, which arises due to the decay of the forward-going ρ^0 meson in the nucleus. This ρ meson is assumed to be produced coherently in the (p, p') reaction on a nucleus. The coherent meson production process ensures that the recoil nucleus remains in the

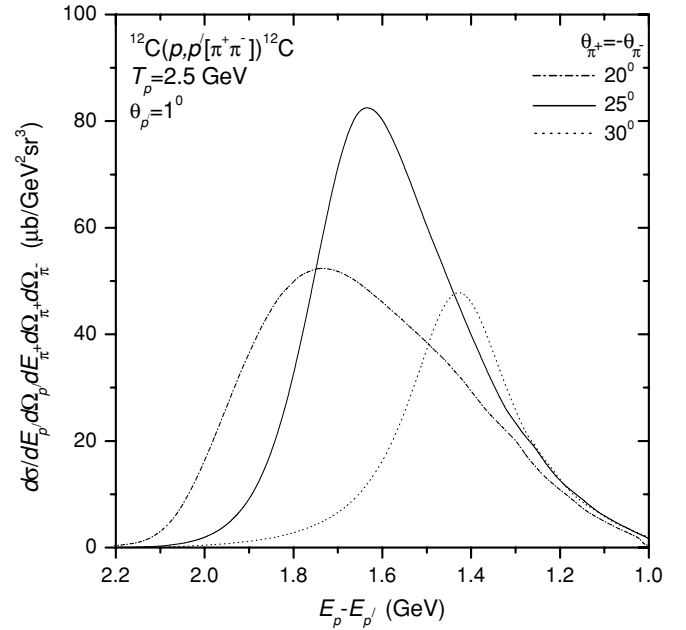


FIG. 1. Sensitivity of the energy transfer $E_p - E_{p'}$ distribution spectrum to the pion emission angle. The peak cross section is maximum for the π^+ emission angle taken equal to 25° . The peak position is shifted toward the lower value of $E_p - E_{p'}$ with an increase in the pion emission angle.

same state as the target nucleus. The forward propagation of the ρ^0 meson, considered here for simplicity, imposes a constraint on the pion emission angle: $\theta_{\pi^+} = -\theta_{\pi^-}$. In these calculations, the p' emission angle is fixed at 1° .

For the above reaction on the ^{12}C nucleus, the sensitivity of the cross section to the pion emission angle is presented in Fig. 1 at 2.5 GeV beam energy. The cross sections have been calculated for various π^+ emission angles θ_{π^+} taken sequentially from 5° to 35° . In Fig. 1, we show the calculated results only for θ_{π^+} taken equal to 20° , 25° , and 30° . This figure shows that the peak position is shifted toward the lower value of $E_p - E_{p'}$ with the increase in the π^+ emission angle. It also shows that the cross section is maximum for the π^+ emission angle of 25° . For this angle, the cross section at the peak is $82.5 \mu\text{b}/(\text{GeV}^2 \text{sr}^3)$, which appears at the energy transfer $E_p - E_{p'} = 1.64 \text{ GeV}$. The peak cross section for $\theta_{\pi^+} = 20^\circ$ is $52.35 \mu\text{b}/(\text{GeV}^2 \text{sr}^3)$, appearing at $E_p - E_{p'} = 1.74 \text{ GeV}$, whereas the cross section at the peak for $\theta_{\pi^+} = 30^\circ$ is about $48 \mu\text{b}/(\text{GeV}^2 \text{sr}^3)$, and it appears at $E_p - E_{p'} = 1.43 \text{ GeV}$.

In nuclear reactions it is often seen that the cross section strongly depends on the beam energy. To show this dependence, the energy transfer $E_p - E_{p'}$ distribution spectra have been calculated for the above reaction at beam energies taken equal to 2.5, 3, and 3.5 GeV. The π^+ emission angle θ_{π^+} is fixed at 25° , since this setting, as shown in Fig. 1, gives the maximum cross section at 2.5 GeV beam energy. The calculated $E_p - E_{p'}$ distribution spectra are presented in Fig. 2, which shows the cross section increases with the increase in beam energy. The cross section at the peak is enhanced to $0.75 \text{ mb}/(\text{GeV}^2 \text{sr}^3)$ at 3.5 GeV from $82.5 \mu\text{b}/(\text{GeV}^2 \text{sr}^3)$ at 2.5 GeV. The peak position at 3.5 GeV beam energy appears

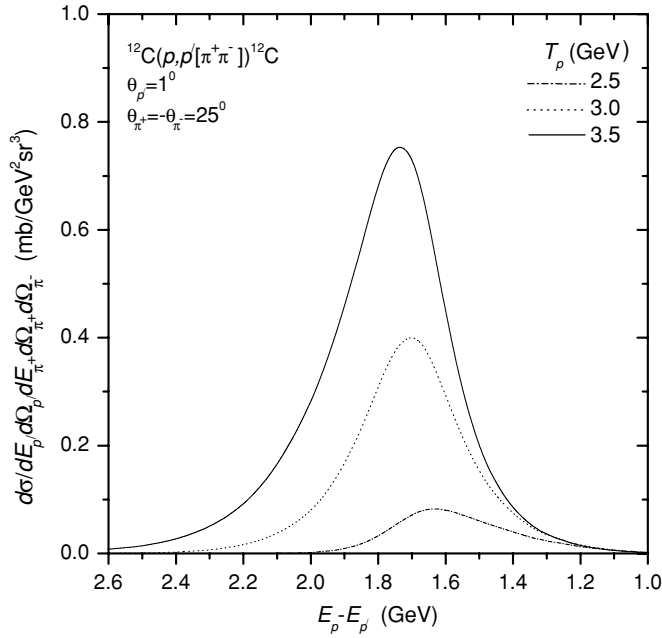


FIG. 2. Dependence of the energy transfer $E_p - E_{p'}$ distribution spectrum on the beam energy. With an increase in the beam energy, the cross section increases and the peak position moves toward the higher value of $E_p - E_{p'}$. The π^+ emission angle is fixed at 25° (see text).

at $E_p - E_{p'} = 1.74$ GeV, where as it appears at $E_p - E_{p'} = 1.64$ GeV for the beam energy taken equal to 2.5 GeV. At 3 GeV, the calculated cross section at the peak is 0.4 mb/(GeV² sr³), and it appears at $E_p - E_{p'} = 1.7$ GeV.

An unstable particle, while propagating through a nucleus, can decay inside as well as outside the nucleus, depending on its velocity and the size of the nucleus. To explore this possibility for the ρ^0 meson propagating through the ^{12}C nucleus, the cross sections for the inside and the outside decay probabilities have been compared in Fig. 3 at 3.5 GeV beam energy. The π^+ emission angle is taken equal to 20° , since it gives the maximum cross section (not shown) at 3.5 GeV beam energy. The peak cross section for the ρ meson decaying inside of this nucleus is 0.12 mb/(GeV² sr³), appearing at $E_p - E_{p'} = 1.98$ GeV (dotted curve), whereas it is equal to ~ 1.46 mb/(GeV² sr³) at $E_p - E_{p'} = 2.12$ GeV for ρ^0 decaying outside the same nucleus (dashed curve). Therefore, the outside decay cross section for this reaction dominates by a factor of about 12 over the inside decay cross section. This figure also compares the coherent and the incoherent contributions to the cross section, coming from the inside and the outside decay amplitudes for ρ^0 traveling through the ^{12}C nucleus. As illustrated in this figure, the peak cross section due to the incoherent contribution is about 1.57 mb/(GeV² sr³) at $E_p - E_{p'} = 2.12$ GeV (dashed-dotted line). On the other hand, it is ~ 2.17 mb/(GeV² sr³) due to coherent contribution, appearing at $E_p - E_{p'} = 2.08$ GeV (solid curve). Therefore, the coherent contribution supercedes the incoherent contribution by a factor of about 1.4.

The inside decay probability for the ρ meson should increase while it propagates through a larger nucleus. To show

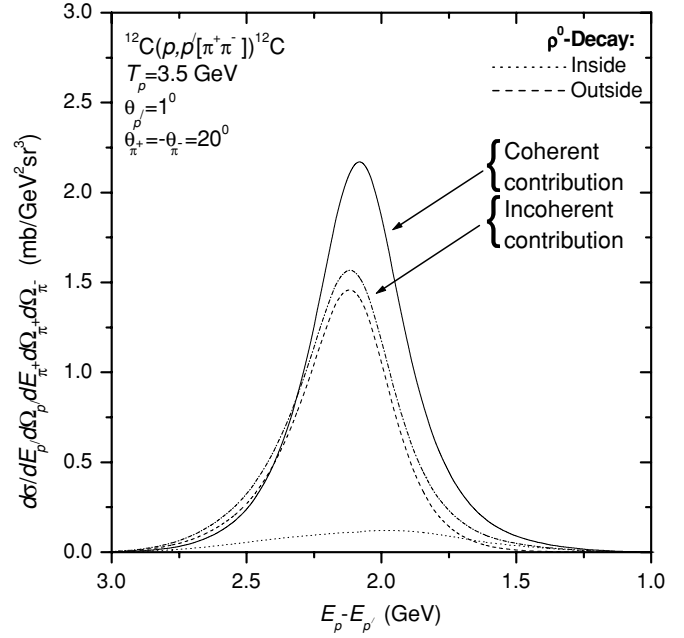


FIG. 3. Cross sections for the ρ meson decaying inside and outside the nucleus are compared for the ^{12}C nucleus at 3.5 GeV beam energy. The outside decay cross section dominates for this nucleus. The interference between the inside and the outside decay amplitudes enhances the cross section. The various curves are explained in the text.

this, the cross sections for the ρ^0 meson decaying inside and outside the ^{208}Pb nucleus have been calculated at 3.5 GeV beam energy. The π^+ emission angle is taken at 15° in this case, since it gives maximum cross section for the Pb target. The calculated results are presented in Fig. 4. It is noticeable in this figure that the peak cross sections for the inside and the outside decay probabilities of the ρ^0 meson, traveling through the Pb nucleus, are comparable with each other [~ 65 $\mu\text{b}/(\text{GeV}^2 \text{sr}^3)$], unlike the case for the ^{12}C nucleus (see Fig. 3). Another remarkable aspect of this figure is the enhancement in the cross section due to the interference between the inside and the outside decay amplitudes for the ρ^0 meson. The peak cross section due to incoherent contribution is 0.11 mb/(GeV² sr³) at $E_p - E_{p'} = 2.2$ GeV (dashed-dotted curve), whereas, that due to the coherent contribution is equal to 0.22 mb/(GeV² sr³), appearing at $E_p - E_{p'} = 2.19$ GeV (solid curve). Therefore, the interference effect enhances the cross section over the incoherent contribution by a factor of 2 for the Pb nucleus, which is significantly larger than that for the C nucleus.

It is always very interesting to investigate the initial- and final-state interactions in the nuclear reactions. The effect of these interactions on the $\pi^+\pi^-$ emission in the (p, p') reaction in the ^{12}C nucleus is shown in Fig. 5 at 3.5 GeV beam energy. This figure compares the calculated distorted-wave results for the continuum particles (i.e., p, p', π^+ , and π^-) with the plane-waves results. In addition, the nuclear effect on the ρ propagation through the ^{12}C nucleus is also presented. The plane-wave result (which also includes the free ρ^0 propagator)

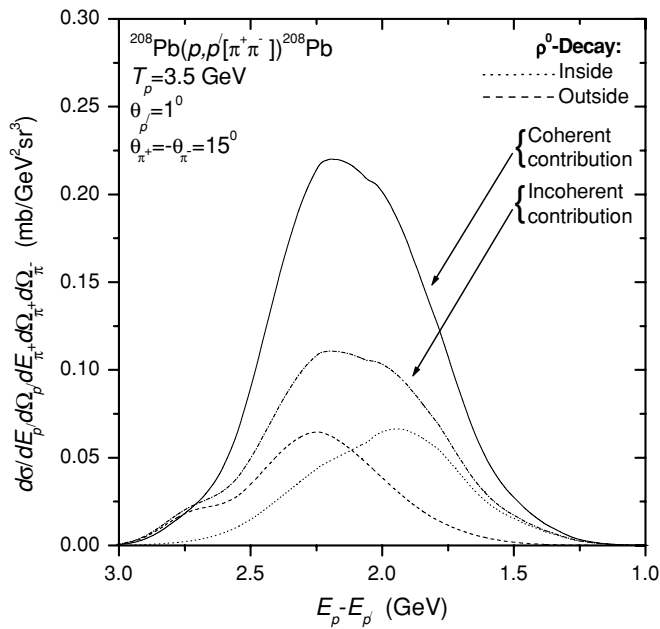


FIG. 4. Inside and outside decay cross sections for the ρ meson propagating through the ^{208}Pb nucleus. The inside decay cross section is substantially increased for the heavier nucleus. In this case, the interference due to the ρ^0 inside and outside decay amplitudes is stronger than that for the ^{12}C nucleus.

shows that the cross section is $25.54 \text{ mb}/(\text{GeV}^2 \text{ sr}^3)$ at the peak, appearing at $E_p - E_{p'} = 2.02 \text{ GeV}$ (dashed-double-dotted curve). The distortion due to the projectile proton p brings down the peak cross section to $7.02 \text{ mb}/(\text{GeV}^2 \text{ sr}^3)$ at

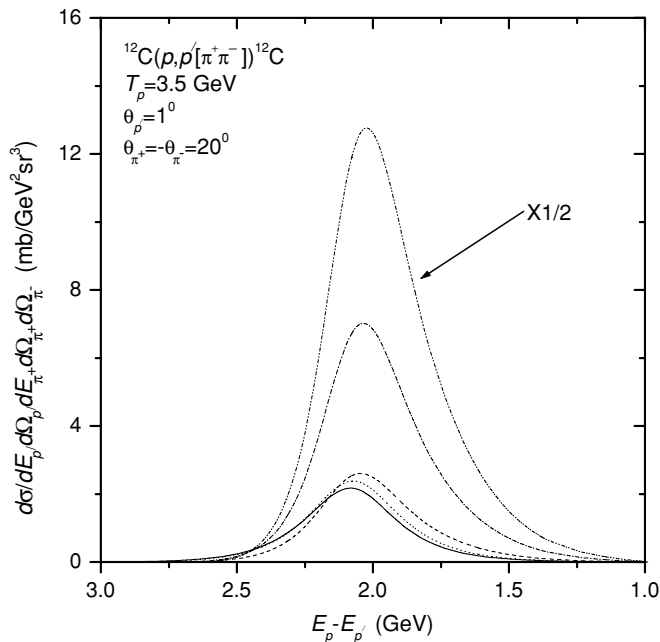


FIG. 5. Effect of the initial- and the final-state interactions on the cross section, for the $(p, p'[\pi^+\pi^-])$ reaction on the ^{12}C nucleus. The beam energy is taken equal to 3.5 GeV . The nuclear effect on the ρ propagation is also presented. The various curves are described in the text.

$E_p - E_{p'} = 2.04 \text{ GeV}$ (dashed-dotted curve). Therefore, the initial-state interaction reduces the cross section by a factor of about 3.64 at the peak, and it shifts the peak position by 20 MeV toward the higher side in the $E_p - E_{p'}$ distribution spectrum. The incorporation of the distortion due to ejectile proton p' further attenuates the peak cross section to $2.6 \text{ mb}/(\text{GeV}^2 \text{ sr}^3)$ at $E_p - E_{p'} = 2.05 \text{ GeV}$ (dashed curve). Therefore, the projectile and ejectile (i.e., p and p') distortions together reduce the plane-wave cross section by a factor of about 9.82 at the peak, and they shift the peak position by 30 MeV toward the higher value of $E_p - E_{p'}$. The final-state interactions due to $\pi^+\pi^-$ together shift the peak position to $E_p - E_{p'} = 2.07 \text{ GeV}$, leaving the magnitude of the peak cross section [$\sim 2.38 \text{ mb}/(\text{GeV}^2 \text{ sr}^3)$] almost unaffected (dotted curve). Therefore, the overall final-state interactions reduce the cross section by a factor of about 2.95 at the peak, and they shift the peak position by 30 MeV toward the higher side in the $E_p - E_{p'}$ distribution spectrum. The initial- and final-state interactions together, as shown in Fig. 5, bring down the plane-wave cross section by a factor of ~ 10.7 at the peak, and they also shift the peak position by 50 MeV toward the higher value in the $E_p - E_{p'}$ distribution spectrum. The ρ^0 nucleus interaction (which appears in the ρ meson propagator) is found not much sensitive to the cross section. It attenuates the peak cross section by only about 8.8%, i.e., from $2.38 \text{ mb}/(\text{GeV}^2 \text{ sr}^3)$ to $2.17 \text{ mb}/(\text{GeV}^2 \text{ sr}^3)$, and it shifts the peak position by 10 MeV to $E_p - E_{p'} = 2.08 \text{ GeV}$ (solid curve).

The initial- and final-state interactions could be very intensive for those nuclear reactions, which involve heavier nuclei. For illustration, the calculated plane- and distorted-wave results for the Pb nucleus are presented in Fig. 6. As exhibited in this figure, the plane-wave results (which also incorporate

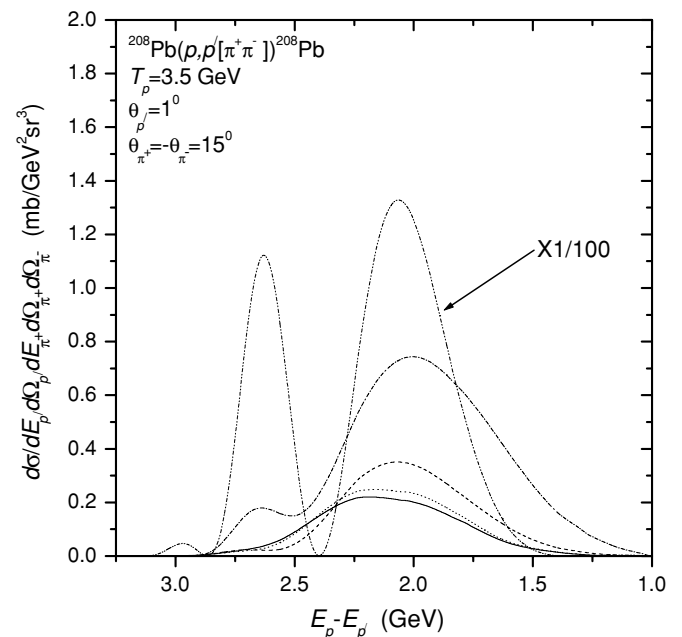


FIG. 6. Initial- and final-state interactions arising due to the ^{208}Pb nucleus. Compared with those for the ^{12}C nucleus, these interactions are more intense. The various curves are defined in the text.

the free ρ^0 propagator) show oscillations in the energy transfer $E_p - E_{p'}$ spectrum (dashed-double-dotted curve), which arise owing to the oscillatory nature of the form factor for the Pb nucleus. The initial-state interaction reduces this oscillation drastically, showing a prominent peak at 2.01 GeV in the energy transfer $E_p - E_{p'}$ spectrum (dashed-dotted curve). The cross section at this peak is about 0.74 (mb/GeV² sr³). Therefore, the initial-state interaction alone brings down the cross section at the main peak by a factor of about 179, and it shifts the peak position by 50 MeV toward the lower value of $E_p - E_{p'}$. The incorporation of p' distortion reduces the peak cross section further to 0.35 mb/(GeV² sr³), at $E_p - E_{p'}$ equal to 2.07 GeV (dashed curve). Therefore, the projectile and ejectile (i.e., p and p') distortions together attenuate the cross section at the main peak by a factor of about 379 and shift the peak position by 10 MeV only toward the higher side in the $E_p - E_{p'}$ distribution spectrum. The final-state interactions due to $\pi^+\pi^-$ together flatten the peak considerably, and they further reduce the peak cross section to ~ 0.25 mb/(GeV² sr³) (dotted curve). Therefore, the final-state interactions altogether bring down the cross section by a factor about 3. In this case, the ρ nucleus interaction reduces the cross section by 12%,

i.e., from 0.25 mb/(GeV² sr³) to 0.22 mb/(GeV² sr³), leaving the shape for the spectrum unchanged (solid curve).

IV. CONCLUSION

This study shows that the cross section for the $\pi^+\pi^-$ emission from the forward-going coherent ρ^0 meson, produced in the (p, p') reaction, reaches its maximum value for a certain direction of the pion emission. The cross section strongly depends on the beam energy. The probability for the ρ meson decaying inside the nucleus is less for a lighter nucleus. It increases with the size of the nucleus. However, the interference between the inside and the outside decay amplitudes for the ρ meson is very important in evaluating the cross section. The initial- and final-state interactions significantly dampen the plane-wave cross section, which is a drastic effect for the heavier nucleus.

ACKNOWLEDGMENT

I gratefully thank A. K. Mohanty for his encouragement.

-
- [1] A. Drees, Nucl. Phys. **A610**, 536c (1996); CERES Collaboration, Th. Ullrich, *ibid.* **A610**, 317c (1996); HELIOS-3 Collaboration, M. Maser, *ibid.* **A590**, 93c (1995); NA50 Collaboration, E. Scomparin, *ibid.* **A610**, 331c (1996).
- [2] G. Q. Li, C. M. Ko, and G. E. Brown, Phys. Rev. Lett. **75**, 4007 (1995); G. Q. Li, C. M. Ko, G. E. Brown, and H. Sorge, Nucl. Phys. **A611**, 539 (1996); W. Cassing, W. Ehehalt, and C. M. Ko, Phys. Lett. **B363**, 35 (1995); W. Cassing, W. Ehehalt, and I. Kralik, *ibid.* **B377**, 5 (1996).
- [3] G. Chanfray, R. Rapp, and J. Wambach, Phys. Rev. Lett. **76**, 368 (1996); R. Rapp, G. Chanfray, and J. Wambach, Nucl. Phys. **A617**, 472 (1997); W. Cassing, E. L. Bratkovskaya, R. Rapp, and J. Wambach, Phys. Rev. C **57**, 916 (1998); R. Rapp and J. Wambach, Eur. Phys. J. A **6**, 415 (1999).
- [4] J. Adams *et al.*, Phys. Rev. Lett. **92**, 092301 (2004).
- [5] G. E. Brown and M. Rho, Phys. Rev. Lett. **66**, 2720 (1991).
- [6] T. Hatsuda and S. H. Lee, Phys. Rev. C **46**, R34 (1992).
- [7] M. Asakawa, C. M. Ko, P. Lévai, and X. J. Qiu, Phys. Rev. C **46**, R1159 (1992); M. Asakawa and C. M. Ko, *ibid.* **48**, R526 (1993); Nucl. Phys. **A560**, 399 (1993).
- [8] K. Saito, K. Tsushima, and A. W. Thomas, Phys. Rev. C **55**, 2637 (1997); **56**, 566 (1997).
- [9] B. Friman, Nucl. Phys. **A610**, 358c (1996); B. Friman and H. J. Pirner, *ibid.* **A617**, 496 (1997).
- [10] W. Peters, M. Post, H. Lenske, S. Leupold, and U. Mosel, Nucl. Phys. **A632**, 109 (1998); M. Post, S. Leupold, and U. Mosel, *ibid.* **A689**, 753 (2001).
- [11] M. Herrmann, B. L. Friman, and W. Nörenberg, Z. Phys. A **343**, 119 (1992); Nucl. Phys. **A560**, 411 (1993).
- [12] C. M. Ko, V. Koch, and G. Li, Annu. Rev. Nucl. Part. Sci. **47**, 505 (1997); W. Cassing and E. L. Bratkovskaya, Phys. Rep. **308**, 65 (1999); R. Rapp and J. Wambach, Adv. Nucl. Phys. **25**, 1 (2000).
- [13] D. Heddle and B. M. Preedom, Spokespersons, "Nuclear mass dependence of vector meson using the photoproduction of lepton pairs," CEBAF proposal PR 89-001 (unpublished); P. Y. Bertin, M. Kosssov, and B. M. Preedom, Spokespersons, "Photoproduction of vector meson off nuclei," CEBAF Proposal PR 94-002 (unpublished).
- [14] "Current experiments in elementary particle physics," Reports INS-ES-134 and INS-ES-144, LBL-91 revised, UC-414, 1994 p. 108 (unpublished); K. Maruyama, in *Proceedings of the 25th International Symposium on Nuclear and Particle Physics with High Intensity Proton Accelerators* (World Scientific, Singapore, 1998); Nucl. Phys. **A629**, 351c (1998).
- [15] CBELSA/TAPS Collaboration, D. Trnka *et al.*, Phys. Rev. Lett. **94**, 192303 (2005).
- [16] R. Muto *et al.*, J. Phys. G: Nucl. Part. Phys. **30**, S1023 (2004).
- [17] H. En'yo *et al.*, KEK Experiment E325; S. Yokkaichi *et al.*, KEK-PS E325 Collaboration, Nucl. Phys. **A638**, 435c (1998).
- [18] HADE Collaboration, W. Koenig, in *Proceedings of the Workshop on Dilepton Production in Relativistic Heavy Ion Collisions*, edited by H. Bokemeyer (GSI, Darmstadt, 1994), p. 225; HADE Proposal, R. Schicker *et al.*, Nucl. Instrum. Methods A **380**, 586 (1996); J. Friese, Prog. Part. Nucl. Phys. **42**, 235 (1999).
- [19] M. Fujiwara, Prog. Part. Nucl. Phys. **50**, 487 (2003).
- [20] V. L. Eletsky and B. L. Ioffe, Phys. Rev. Lett. **78**, 1010 (1997); V. L. Eletsky, B. L. Ioffe, and J. I. Kapusta, Eur. Phys. J. A **3**, 381 (1998).
- [21] L. A. Kondratyuk, A. Sibirtsev, W. Cassing, Ye. S. Golubeva, and M. Effenberger, Phys. Rev. C **58**, 1078 (1998).
- [22] M. Effenberger, E. L. Bratkovskaya, and U. Mosel, Phys. Rev. C **60**, 044614 (1999).
- [23] Th. Weidmann, E. L. Bratkovskaya, W. Cassing, and U. Mosel, Phys. Rev. C **59**, 919 (1999); M. Effenberger,

- E. L. Bratkovskaya, W. Cassing, and U. Mosel, *ibid.* **60**, 027601 (1999).
- [24] Ye. S. Golubeva, L. A. Kondratyuk, and W. Cassing, Nucl. Phys. **A625**, 832 (1997).
- [25] D. Cabrera and M. J. Vicente Vacas, Phys. Rev. C **67**, 045203 (2003); D. Cabrera, L. Roca, E. Oset, H. Toki, and M. J. Vicente Vacas, Nucl. Phys. **A733**, 130 (2004); V. K. Magas, L. Roca, and E. Oset, Phys. Rev. C **71**, 065202 (2005).
- [26] T. Ericson and W. Weise, *Pions and Nuclei* (Clarendon, Oxford, 1988).
- [27] E. Oset, H. Toki, and W. Weise, Phys. Rep. **83**, 281 (1982); C. Gaarde, Annu. Rev. Nucl. Part. Sci. **41**, 187 (1991).
- [28] I. Laktineh, W. M. Alberico, J. Delorme, and M. Ericson, Nucl. Phys. **A555**, 237 (1993); R. C. Carrasco, J. Nieves, and E. Oset, *ibid.* **A565**, 797 (1993); B. Krusche *et al.*, Phys. Lett. **B526**, 287 (2002); D. Drechsel, L. Tiator, S. S. Kamalov, and S. N. Yang, Nucl. Phys. **A660**, 423 (1999); R. J. Loucks and V. R. Pandharipande, Phys. Rev. C **54**, 32 (1996); M. J. M. van Sambeek *et al.*, Nucl. Phys. **A631**, 545c (1998).
- [29] J. Chiba *et al.*, Phys. Rev. Lett. **67**, 1982 (1991); T. Hennino *et al.*, Phys. Lett. **B303**, 236 (1993).
- [30] V. F. Dmitriev, Phys. Rev. C **48**, 357 (1993); P. Oltmanns, F. Osterfeld, and T. Udagawa, Phys. Lett. **B299**, 194 (1993); F. Osterfeld, B. K rfggen, P. Oltmanns, and T. Udagawa, Phys. Scr. **48**, 95 (1993); T. Udagawa, P. Oltmanns, F. Osterfeld, and S. W. Hong, Phys. Rev. C **49**, 3162 (1994); B. K rfggen, F. Osterfeld, and T. Udagawa, *ibid.* **50**, 1637 (1994); P. F. de C rdoba, J. Nieves, E. Oset, and M. J. Vicente-Vacas, Phys. Lett. **B319**, 416 (1993); E. Oset, P. F. de C rdoba, J. Nieves, and M. J. Vicente-Vacas, Phys. Scr. **48**, 101 (1993); P. F. de C rdoba, E. Oset, and M. J. Vicente-Vacas, Nucl. Phys. **A592**, 472 (1995).
- [31] R. Machleidt, Adv. Nucl. Phys. **19**, 189 (1989).
- [32] R. K. Bhaduri, *Models of the Nucleon* (Addison-Wesley, Reading, Mass, 1988).
- [33] S. Das, Phys. Rev. C **70**, 034604 (2004); B. K. Jain and Bijoy Kundu, *ibid.* **53**, 1917 (1996).
- [34] H. De. Vries and C. W. De Jager, At. Data Nucl. Data Tables **14**, 479 (1974).
- [35] D. V. Bugg *et al.*, Phys. Rev. **146**, 980 (1966); S. Barshay *et al.*, Phys. Rev. C **11**, 360 (1975); W. Grein, Nucl. Phys. **B131**, 255 (1977); C. Lechanoine-LeLue, Rev. Mod. Phys. **65**, 47 (1993).
- [36] Particle Data Group, Phys. Rev. D **54**, 1 (1996).
- [37] R. A. Arndt *et al.*, SAID Programme, <http://gwdac.phys.gwu.edu>.
- [38] M. F. M. Lutz, Gy. Wolf, and B. Friman, Nucl. Phys. **A706**, 431 (2002).